An Introduction to Single Crystal Perovskites and Single Crystal Rare-Earth Scandate Perovskites Analyzed Using X-ray Photoelectron Spectroscopy

Richard T. Haasch, Eric Breckenfeld, and Lane W. Martin

An Introduction to Single Crystal Perovskites and Single Crystal Rare-Earth Scandate Perovskites Analyzed Using X-ray Photoelectron Spectroscopy

Richard T. Haasch
Department of Materials Science and Engineering and Materials Research Laboratory,
University of Illinois, Urbana-Champaign, Illinois 61810

Eric Breckenfeld
Department of Materials Science and Engineering and Materials Research Laboratory,
University of Illinois, Urbana-Champaign, Illinois 61801; and Naval Research Laboratory,
Washington, DC 20375

Lane W. Martin
Department of Materials Science and Engineering and Materials Research Laboratory,
University of Illinois, Urbana-Champaign, Illinois 61801; Department of Materials Science
and Engineering, University of California, Berkeley, California 94720; and Materials Science Division,
Lawrence Berkeley National Laboratory, Berkeley, California 94720

Oxides of transition and inner transition metals show a variety of technologically important functional properties. Among these properties include ferroelectricity[1] and magnetism,[2] colossal magnetoresistance,[3] and high temperature superconductivity,[4] with transport character ranging from insulating to semiconducting to metallic. Furthermore, these properties are extremely sensitive to perturbations from chemistry, structural defects, strain, and many other effects, which, in turn, provides the materials scientist a number of routes by which to engineer new functionalities in this class of materials.[5] While even simple binary oxide systems exhibit a broad diversity of properties, it is the ternary systems that have received the most attention in recent years. In particular, materials possessing the perovskite structure [with chemical formula ABO_3 (Fig. 1)] have been observed to exhibit an incredible variety of functionality and phenomena.

This paper introduces two sets of five Surface Science Spectra comparison data records: (1). Single crystal perovskites analyzed using X-ray photoelectron spectroscopy, which include $SrTiO_3$ (001), $YAlO_3$ (110), $LaAlO_3$ (001), $(LaAlO_3)_{0.3}(Sr_2TaAlO_6)_{0.7}$ (001), and $NdGaO_3$ (110); (2) Single crystal rare-earth scandate perovskites analyzed using X-ray photoelectron spectroscopy, which include $PrScO_3$ (110), $NdScO_3$ (110), $GdScO_3$ (110), $TbScO_3$ (110), and $DyScO_3$ (110). Although there are many interesting aspects of the perovskites and rare-earth scandate perovskites, this very brief introduction will touch on their use as substrates for epitaxial growth, and the electronic effects of these materials on the lanthanide metal 3d photoelectron spectra. Other work relating to lanthanide-based materials has appeared previously in Surface Science Spectra.[6]

The perovskite structure generally involves a larger metal cation, A, together with a smaller metal cation B (Fig. 1).[7] The ideal symmetry of a perovskite is cubic. The relative size of the two cations is crucial for stability of the cubic structure and variations in ionic radius of either the A or B cation or both can lead to crystal distortion affecting not only the overall crystal structure but also the electronic structure and properties as well. This makes perovskites an interesting class of materials not only for their functional properties, but also as substrates for epitaxial growth.
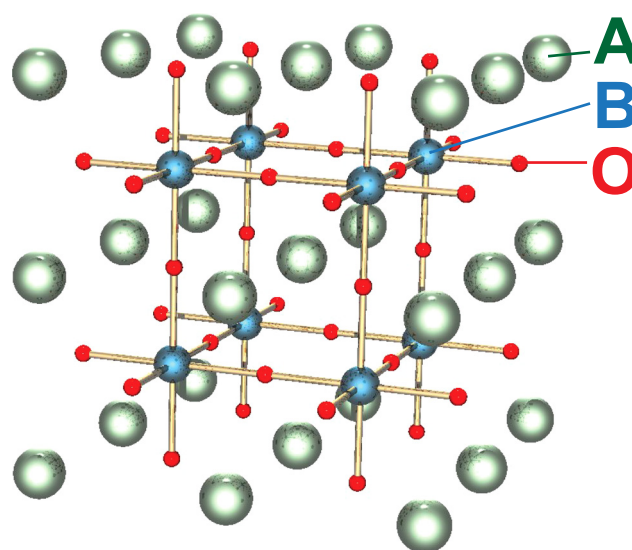
FIG. 1. Perovskite (ABO_3) structure.

TABLE I. Crystal ionic radii (Ref. 12).

A		B	
Ion	Radius (nm)	Ion	Radius (nm)
Sr^{3+}	0.132	Al^{3+}	0.0675
Y^{3+}	0.104	Sc^{3+}	0.0885
La^{3+}	0.1172	Ti^{3+}	0.081
Pr^{3+}	0.113	Ga^{3+}	0.076
Nd^{3+}	0.1123	Ta^{3+}	0.072
Gd^{3+}	0.1078		
Tb^{3+}	0.1063		
Dy^{3+}	0.1052		
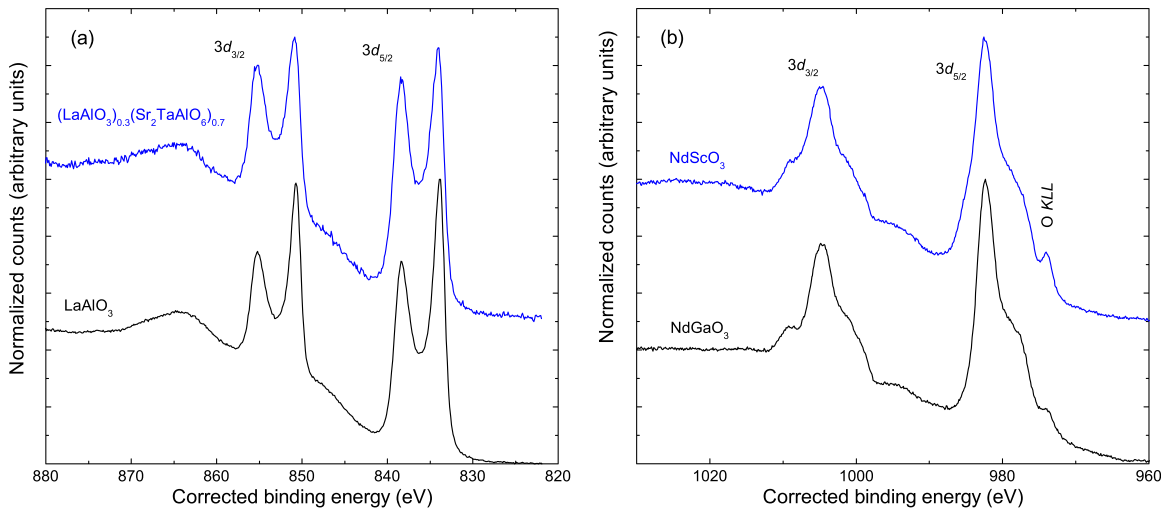
Fig. 2. (a) La 3d photoelectron spectra of $LaAlO_3$ (001) and $(LaAlO_3)_{0.3}(Sr_2TaAlO_6)_{0.7}$ (001). (b) Nd 3d photoelectron spectra of $NdGaO_3$ (110) and $NdScO_3$ (110).

Advances in thin film epitaxy, particularly pulsed laser deposition, RF magnetron sputtering, and molecular beam epitaxy, have enabled researchers to carefully tune material properties using epitaxial strain, either induced by compositional variation or by substrate variation taking advantage of lattice mismatch. Such approaches have provided an opportunity for researchers growing perovskite thin films or making use of single crystal perovskites as substrates for epitaxial growth to apply large biaxial strains (as much as several percent in some cases) to nanoscale films of various materials, which would lead to cracks in bulk materials under similar values of hydrostatic strain.[8] In order to gain an increased understanding of the surfaces and heterointerfaces of perovskite-based materials, a variety of commercially available bulk single crystalline substrates commonly used for epitaxial growth were chosen in this study, which span a range of crystal ionic radii of A and B (Table I).
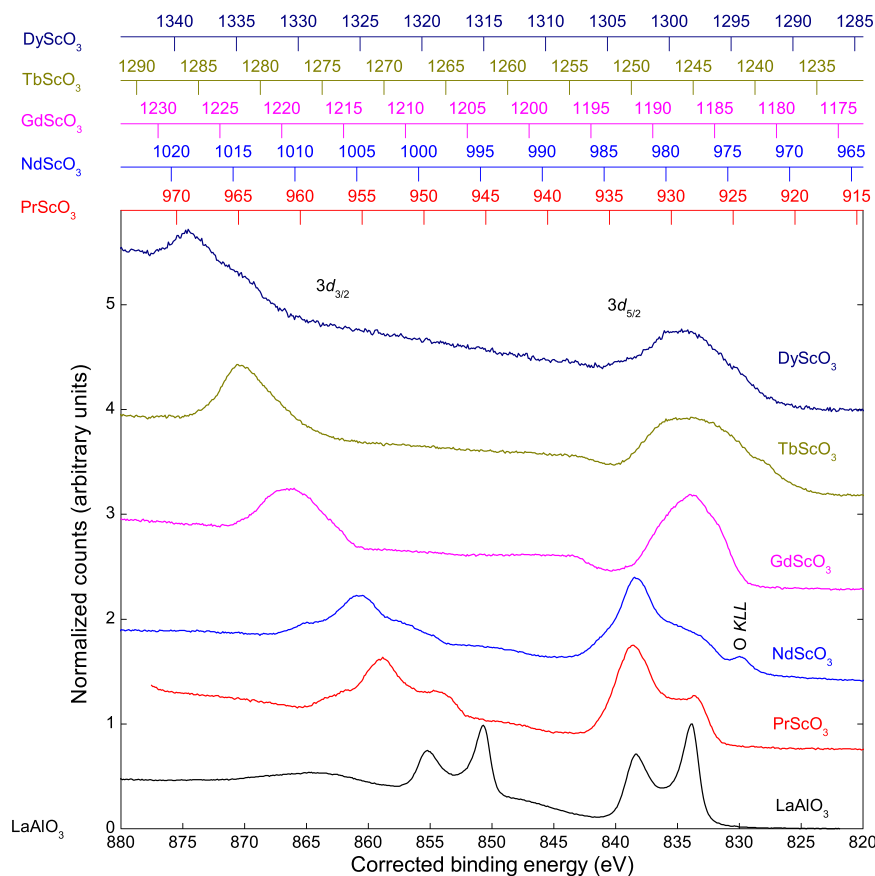
Fig. 3. 3d photoelectron spectra of $LaAlO_3$ (001), $PrScO_3$ (110), $NdScO_3$ (110), $GdScO_3$ (110), $TbScO_3$ (110), and $DyScO_3$ (110).

TABLE II. Electron configuration (Ref. 13).

Element	Electron configuration
La	$[Xe]6s^25d^1$
Pr	$[Xe]6s^24f^3$
Nd	$[Xe]6s^24f^4$
Gd	$[Xe]6s^24f^75d^1$
Tb	$[Xe]6s^24f^9$
Dy	$[Xe]6s^24f^{10}$

The photoelectron spectra of the Al, Sc, Ti, Ga, Sr, and Y species present in the series of perovskite-based materials investigated in this study appear for the most part typical for their +3 state and will not be discussed in detail here. The much more interesting spectra in terms peak-shape complexity are those of the rare-earth elements La, Pr, Nd, Gd, Tb, and Dy present in this series of materials and, in particular, the 3d lines of these elements. The La 3d photoelectron spectra of $LaAlO_3$ (001) and $(LaAlO_3)_{0.3}(Sr_2TaAlO_6)_{0.7}$ (001) in Fig. 2(a) and the Nd 3d photoelectron spectra of $NdGaO_3$ (110) and $NdScO_3$ (110) in Fig. 2(b) each show a double-peak structure characteristic for their respective sesquioxide, La_2O_3 and Nd_2O_3.[9,10] The 3d doublets are quite distinct for $LaAlO_3$ and $(LaAlO_3)_{0.3}(Sr_2TaAlO_6)_{0.7}$ and less distinct for $NdGaO_3$ and $NdScO_3$. For the two lanthanum compounds, the lower binding energy component has nearly the same intensity as the higher binding energy component, whereas for the two Nd compounds, it is the higher binding energy component that dominates. When the ligand is changed, for example, to fluorine, such as in LaF_3, it is the lower binding energy component of the La 3d line that dominates, with the higher binding energy component having diminished intensity as compared to $LaAlO_3$ and $(LaAlO_3)_{0.3}(Sr_2TaAlO_6)_{0.7}$.[11] This indicates the lanthanide-series metal and the ligand anion play key roles in determining the 3d peak shape for this class of materials.

The structure of the 3d lines of the lanthanide series compounds can be explained by a core-hole screening mechanism known as valence-mixing relaxation. During the creation of the core hole, there is a strong coulombic perturbation attracting localized 4f electrons. This causes a relaxation of the 4f charge distribution through hybridization of the 4f electrons with valence (conduction) states in order to screen the core hole.[8,9] For La, Pr, and Nd, each of the states represent either the bonding or the antibonding final state configuration of the metal ion (e.g., for $LaAlO_3$ and $(LaAlO_3)_{0.3}(Sr_2TaAlO_6)_{0.7}$, the higher binding energy line represents the $4f^0\underline{c}$ bonding state and the lower binding energy line is the $4f^1\underline{c}$ anti-bonding state, where $\underline{c}$ represents the

3d core hole.) It is this charge transfer between the metal and ligand that causes the intensity ratios of the double-peak structure to vary by metal and ligand.

The degree of electron interaction varies with the lanthanide element and significantly alters the structure of the 3d spectra as evidenced in Fig. 3. For $LaAlO_3$, the charge-transfer effect is weak, which results in clearly defined doublets for in the 3d lines. For $PrScO_3$ and $NdScO_3$, the charge-transfer effect is strong and the doublet becomes much less clearly defined. This is due in part to an increase in unpaired 4f electrons as these orbitals begin to fill. For $GdScO_3$, $TbScO_3$, and $DyScO_3$, the double-peak structure disappears and the line shape can be explained based on a decrease in the number of unpaired 4f electrons as these orbitals are further filled (Table II).

REFERENCES

1. M. Dawber, K. M. Rabe, and J. F. Scott, Rev. Mod. Phys. **77**, 1083 (2005).
2. S. A. Chambers, T. C. Droubay, C. M. Wang, K. M. Rosso, S. M. Heald, D. A. Schwartz, K. R. Kittilstved, and D. R. Gamelin, Mater. Today **9**, 28 (2006).
3. A. P. Ramirez, J. Phys.: Condens. Matter **9**, 8171 (1997).
4. J.-M. G. Chen Langlois, Y. Guo, and W. A. Goddard III, Proc. Natl. Acad. Sci. U. S. A. **86**, 3447 (1989).
5. D. G. Schlom, L.-Q. Chen, C.-B. Eom, K. M. Rabe, S. K. Streiffffer, and J.-M. Triscone, Ann. Rev. Mater. Res. **37**, 589 (2007).
6. M. M. Natile, Surf. Sci. Spectra **16**, i (2009), and other contributions from this group within Vol. 16.
7. See http://en.wikipedia.org/wiki/Perovskite_(structure)#mediaviewer/File:Perovskite.jpg
8. L. W. Martin and D. G. Schlom, Curr. Opin. Solid State Mater. Sci. **16**, 199 (2012).
9. C. Suzuki, T. Mukoyama, J. Kawai, and H. Adachi, Phys. Rev. B **57**, 9507 (1998).
10. C. Suzuki, J. Kawai, M. Takahashi, A.-M. Vlaicu, H. Adachi, and T. Mukoyama, Chem. Phys. **253**, 27 (2000).
11. J. T. Stecher, A. B. Rohlfing, and M. J. Therien, Nanomaterials **4**, 69 (2014).
12. R. D. Shannon, Acta Cryst. A **32**, 751 (1976).
13. See http://en.wikipedia.org/wiki/Electron_configuration